Emergent Materials (2018) 1:165–173
https://doi.org/10.1007/s42247-018-0015-z

ORIGINAL ARTICLE

# Effect of thermal processing on the tribology of nanocrystalline Ni/$TiO_2$ coatings

Kavian O. Cooke[1,2] · Tahir I. Khan[1]

Received: 14 February 2018 / Accepted: 1 October 2018 / Published online: 18 October 2018


## Abstract

The tribological performance of a nanocrystalline coating is heavily influenced by its composition, morphology, and microstructural characteristics. This research work describes the effect of heat treatment temperature on the microstructural, morphological, and mechanical behavior of nanocrystalline Ni/$TiO_2$ coatings produced by electrophoresis. The surface morphology and coating cross section were characterized by scanning electron microscopy (SEM). The composition of coatings and the percentage of $TiO_2$ nanoparticles incorporated in the Ni matrix were studied and estimated by using an energy-dispersive spectroscopic (EDS) analysis, while x-ray diffractometry (XRD) was used to investigate the effect of heat treatment temperature on phase structure. The results showed agglomeration of $TiO_2$ nanoparticles on the surface of the coating. The high hardness and wear resistance recorded for the as-deposited coating was attributed to the uniform distribution of $TiO_2$ nanoparticle clusters throughout the cross section of the coating. Heat treatment of the Ni/$TiO_2$ coatings to temperatures above 200 °C led to significant grain growth that changed the surface morphology of the coating and reduced the strengthening effects of the nanoparticles, thus causing a reduction in the hardness and wear resistance of the coatings.

**Keywords** Nanocrystalline · Co-electrodeposition · Heat treatment · Sliding wear

## 1 Introduction

Nanostructured cermet coatings have been the focus of several recent studies, because of the possibilities of producing materials with exceptional physical and chemical properties such as superior mechanical, chemical, and tribological properties. The demand for enhanced material performance has led to the development of several nanocomposite coatings capable of achieving certain technological goals [1–4]. According to Wu et al. [5], the improved properties observed in nanocomposite coatings are used extensively in automotive, aerospace, microelectronics, and fuel cell technology [6–12].

There are several techniques capable of producing nanostructured coatings with the required wear and corrosion resistance. Among the available technology, electrophoretic deposition is one of the most economical and flexible techniques for producing wear-resistant coatings [6]. The advantage of electrophoretic deposition is that the process requires simple apparatus and short formation time and can be modified easily for specific applications since the process is not limited by the shape of the material to be coated. In the electrophoretic deposition, charged particles suspended in the electrolyte are attracted to the electrode to be coated due to the difference in polarity between the electrode and the particle [13, 14].

The inclusion of the ceramic particles in the coating and the uniformity of particle distribution are critical to achieving wear-resistant coatings [15–19]. Optimization of the coating parameters can lead to substantial improvements of the coating's wear resistance [20, 21]. The inclusion of nanoparticles in the coating has been shown to significantly improve hardness and other mechanical properties of the coatings [22]. The major challenge, however, is obtaining a uniform distribution of the ceramic particles in the coating. The volume of the particles embedded in the coating is dependent on the concentration of ceramic particles suspended in the solution; therefore, as particle concentration in the solution increases, the volume of particles embedded in the coating also increases. Other factors such as surfactant concentration and zeta

✉ Kavian O. Cooke
kavian_cooke@yahoo.com

[1] Faculty of Engineering and Informatics, University of Bradford, Richmond Road, Bradford BD7 1DP, UK

[2] School of Engineering, University of Technology, 237 Old Hope Road, Kingston, WI, Jamaica

potential have also been shown to affect the volume of particle deposited [23, 24].

The incorporated particles act as barriers to dislocation motion which strengthens the material as predicted by Orowan's dispersion strengthening theory. The strength of the composite is expected to increase as the size and inter-particle spacing of the dispersed particles decrease [25]. Additionally, the incorporation of nanosized particles may also cause grain size reduction leading to further strengthening of the coatings, as predicted by the Hall-Petch relationship [26].

Although several researchers have attempted to map the wear behavior of the as-deposited nanocomposite cermet coatings produced by electrophoretic deposition, there is still a gap in the scientific literature on the impact of heat treatment temperatures on the tribological performance of nanocrystalline materials produced by electrophoresis. This study bridges the gap in the literature by evaluating the effect of heat treatment temperature on the thermal stability, microhardness, and sliding wear performance of $Ni/TiO_2$ nanocrystalline coating produced by electrophoretic deposition. The results of the study allow for the determination of operational limits for $Ni/TiO_2$ nanocrystalline coatings.

## 2 Experimental procedure

### 2.1 Electrodeposition

The nanocrystalline cermet coatings were deposited from Watt's nickel bath solution containing anatase $TiO_2$ nanoparticles. The bath composition and the volume of oxide particles (20 g/L) used were obtained from previous research [14]. A 99.5% pure nickel plate was used as the anode, and an AISI1020 carbon steel of dimension 25.4 mm × 20 mm × 10 mm was used as the cathode. The distance between the anode and cathode was maintained at approximately 2 cm during the deposition process. The electrodeposition process was carried out in a 250-mL beaker at 50 °C using a current density of 5A/$dm^2$ and magnetic stirring of 250 rpm for 30 min, to prevent particle agglomeration during deposition. These parameters were selected to comply with the optimized values published in previous studies [14, 19].

The anatase $TiO_2$ nanopowders having a particle size of 40 nm were obtained from Good-fellow (Cambridge UK). Prior to the deposition process, the steel substrates were prepared using abrasive papers (240, 400, 600, and 1200 grit) and polished to 1 μm using a particle impregnated carrier paste. The samples were subsequently decreased with acetone and rinsed with deionized water. After the coating process, the cathode was extracted from the cell and rinsed with deionized water.

### 2.2 Hardness

Microhardness tests were performed on the coating cross section using a Leitz microhardness tester to record ten indentations using a 0.1-kg load applied for 30 s. Subsequently, the average Vickers hardness number for the coatings was determined using Eq. 1.

$$HV = 1854.4\,\frac{P}{d^2} \tag{1}$$

where $P$ is the applied load and $d$ is the average of the two diagonals for the recorded indentation.

### 2.3 Thermal processing

The $Ni/TiO_2$ coatings were heat treated in air, using an induction furnace equipped with a temperature control system. A k-type thermocouple was attached to each sample and monitored throughout the heating and cooling process. The heat treatments were conducted according to the conditions outlined in Table 1. The annealing temperatures listed in Table 1 were selected to ensure recrystallization, which has been shown to occur between 320 and 380 °C [26]. The specimens were held at the treatment temperature for 30 min, before the power supply was disconnected and the specimens cooled in air, to room temperature.

### 2.4 Wear testing

The coatings were subjected to two-body abrasive wear tests, and to ensure repeatability, three specimens were heat treated and tested for each test condition. The applied load was varied between 10, 25, and 40 N.

The wear testing was completed using a pin-on-plate test equipped with a diamond pin of diameter 3 mm, mounted in a 90° cone. The pin slides reciprocally against the coated specimen and the wear performance measured by monitoring the changes in the depth of the wear scar as a function of time for 30 min. The tests were conducted under non-lubricating conditions. The changes in the depth of the wear scars were measured before and after the heat treatment. The test data were collected using a 16-bit, 100-kHz data acquisition system.

### 2.5 Microstructural characterization

The morphology of the coating surface and the depth of the wear scars were examined with a Leitz optical microscope and an Oxford scanning electron microscopy (SEM). The concentration of $TiO_2$ nanoparticles deposited in the coating was assessed using energy-dispersive x-ray spectroscopy (EDS). The effect of heat treatment on the crystal structure of the coating was studied using a Bruker x-ray diffractometer

**Table 1** Heat treatment parameters studied

| Parameters | Settings |
|---|---|
| Temperature | 200 °C, 400 °C |
| Heating environment | Air |
| Cooling medium | Air |
| Hold time | 30 min |
| Heating rate | 60 °C/min |

(XRD) equipped with a Cu-Kα radiation. The following settings were used: 40 kV, 40 mA, step size of 0.05° from 2θ ranging from 10 to 100°, and measuring time 1 s per step.

## 3 Results and discussion

This study evaluates the effects of heat treatment temperature on the properties of nanocrystalline Ni/$TiO_2$ coatings and permits a clear understanding of the impact of heat treatment temperature on the strengthening behavior of nanosized $TiO_2$ reinforcements embedded into the coatings. The coatings were characterized for variations in surface morphology, microstructure, hardness, and wear resistance, as the temperature is varied from 200 to 400 °C. The properties and performance of the heat-treated coatings are discussed in this section and compared to the performance of the as-deposited Ni/$TiO_2$ nanocrystalline coatings.

### 3.1 Surface morphology and microstructure

Analysis of the electrodeposited coating by scanning electron microscopy revealed the difference in the surface morphology of heat-treated coatings when compared to the as-deposited coatings. The coating microstructure and surface morphology of the as-deposited Ni/$TiO_2$ nanocrystalline coating is shown in Fig. 1a. It is evident that embedding $TiO_2$ nanoparticles into the coating changes the surface morphology when compared to the smooth surface characteristic of pure nickel coating discussed in previous studies [14]. Spherical asperities are visible on the surface of the coatings with several areas containing clusters indicative of particle agglomerations. The presence of particle clusters changes the morphology of the surface of the coating and is expected to restrict the growth of nickel crystals [27]. While particle agglomeration is possible during electrophoretic deposition, it is likely that the agglomeration observed may have occurred in the as-received powder as discussed in a previous study [28].

The cross section of the Ni/$TiO_2$ nanocomposite coating presented in Fig. 1c shows evidence of spherical agglomerates uniformly distributed throughout the thickness of the coating. Chemical compositional analysis of the cross section using EDS (see Fig. 1d) confirms the presence of nanosized $TiO_2$ particles by a Ti peak and the high oxygen content. The $TiO_2$ content in the cross section of the coating was found to be approximately 16.4 wt%.

The effect of heat treatment temperature on the surface morphology of the Ni/$TiO_2$ is shown in Figs. 2 and 3. From these figures, it was observed that the agglomerations

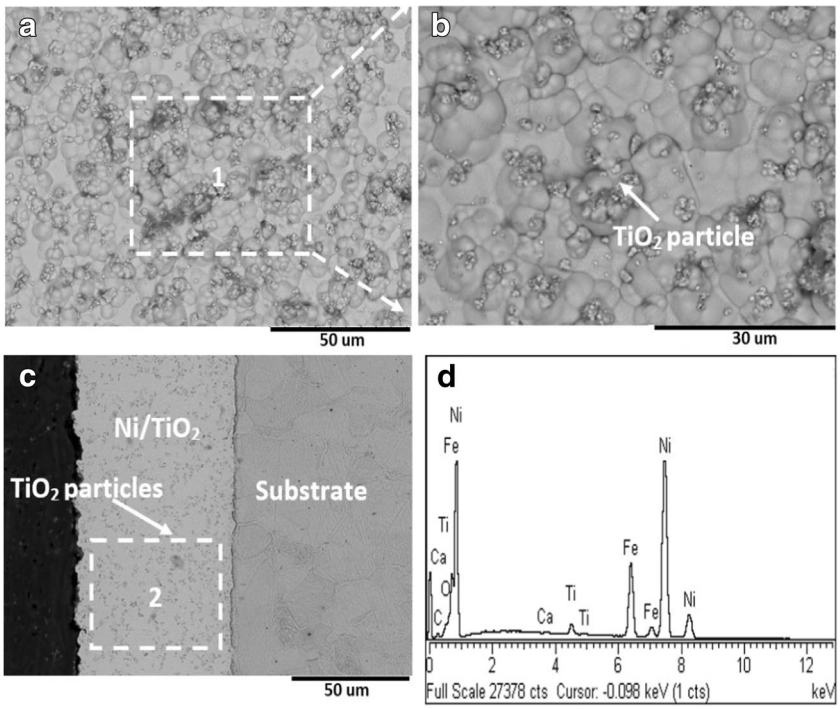


**Fig. 1** **a** The surface morphology of the as-deposited Ni/$TiO_2$ coating. **b** Detail view of region 1. **c** Cross section of Ni/$TiO_2$ coating. **d** EDX analysis of the coating cross section

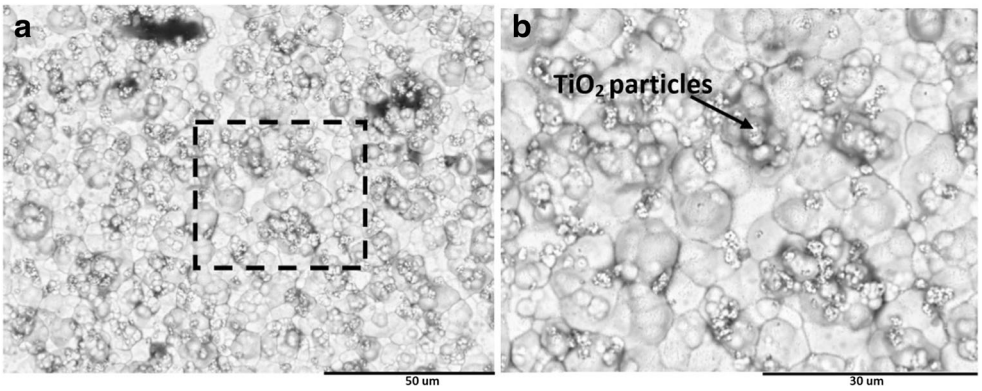


**Fig. 2** **a** SEM micrograph of the $Ni/TiO_2$ coating heat treated to 200 °C. **b** Detail view of the highlighted region

became less pronounce for higher heat treatment temperature. The surface morphology of the $Ni/TiO_2$ coating heat treated to 200 °C is shown in Fig. 2. From the figure, it can be seen that the surface contained particle clusters in the grain boundaries. Additionally, the surface also contained evidence of grain growth, which will be discussed later. When the annealing temperature was further increased to 400 °C, the morphology of the surface changed significantly, with the agglomerations becoming less pronounced, when compared to the surface of the as-deposited coatings (see Fig. 3). The increase of the annealing temperature resulted in grain coarsening, which causes segregation of the nanoparticles to the grain boundary regions [29].

### 3.2 XRD analysis of the crystal structure

X-ray diffraction analyses of the $Ni/TiO_2$ coatings were conducted to identify any phase changes or modification of the diffraction peaks due to heat treatment of the coatings. The XRD spectrums of the coatings produced before and after heat treatment are presented in Fig. 4 and revealed that the peak occurring at 44.3° appeared to decrease in intensity while becoming sharper. The peak found at 78° (220) also appears to increase in intensity. Similar increases were observed in peaks occurring at 92.4° and 97.4°. A peak for nano-$TiO_2$ powders was observed at 25° which decreased in intensity as the annealing temperature increased to 400 °C. The change in the behavior of the coatings, as recorded by the XRD analysis, can be attributed to several factors. The broadness of the XRD peaks recorded for the as-deposited coatings confirms the presence of nanosized $TiO_2$ particles within the coating. The broadness of the XRD peak suggests kinematical scattering, which occurs when crystallites within that material lattice become smaller and are available in sufficiently large enough quantities that the chemical variation across the lattice modifies the XRD spectrum [30]. The presence of nanosized $TiO_2$ particles in the lattices may also induce micro-residual stresses in the as-deposited coatings, which contributes to the hardness of the coating. The modifications of the spectra observed for the heat-treated coatings are caused by intrinsic microstructural changes occurring in the coatings due to grain growth leads to a reduction of the residual stresses within the lattice [27].

### 3.3 Hardness

The microhardness profile for the $Ni/TiO_2$ nanocomposite coating is presented in Fig. 5 and shows the relationship between annealing temperature and microhardness of the $Ni/TiO_2$ coating. The as-deposited $Ni/TiO_2$ coating recorded a microhardness of 663 VHN. However, as the samples are heat treated, the hardness decreased to 600 VHN at 200 °C and 533 VHN at 400 °C respectively. The hardness of the as-deposited $Ni/TiO_2$ is noticeably higher than the heat-treated coatings. The hardness data corroborates the findings from the

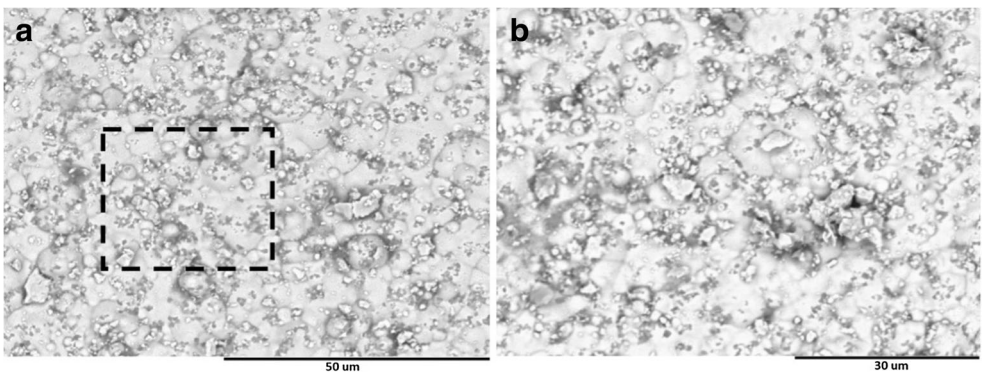


**Fig. 3** **a** SEM micrograph of the $Ni/TiO_2$ coating heat treated to 400 °C. **b** Detail view of the highlighted region

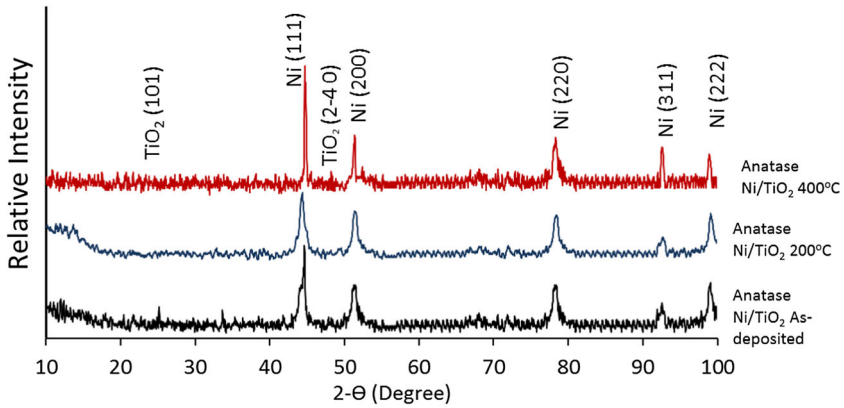


**Fig. 4** XRD spectrum of coatings evaluated $Ni/TiO_2$ coatings evaluated

microstructural and XRD analyses. The reduction in hardness of the coatings was attributed to grain coarsening as the annealing temperature increased. As the grain size increases, the $TiO_2$ nanoparticles are segregated to the grain boundaries became less effective in impeding dislocation motion, and as a result, the hardness of the coatings decreased. In a previous study conducted by Niu et al. [31], the authors evaluated the growth and stability of nanocrystalline $Ni/TiO_2$ composites as a function of the coating composition and annealing temperature. The results of the study confirmed that grain coarsening in nanocomposite coating due to the annealing temperature leads to a steady reduction in the microhardness of the coating.

### 3.4 Sliding wear performance of the coatings

Assessment of the effects of heat treatment on the tribological behavior of the $Ni/TiO_2$ coating was conducted using a reciprocating pin-on-plate wear test. Figure 6 shows the wear profile of the $Ni/TiO_2$ coatings a function of time and load. From the figure, it was observed that the wear of the $Ni/TiO_2$ coating occurred in two stages: firstly, accelerated wear due to the surface morphology of the as-deposited coating, followed by a secondary stage which appears to start after 400 s and can be described as steady-state wear. The changes to the wear rate can be attributed to two factors: firstly, modifications of the height of surface asperities by the reciprocating pin. As the amplitude of surface asperities decreases, the surface roughness also

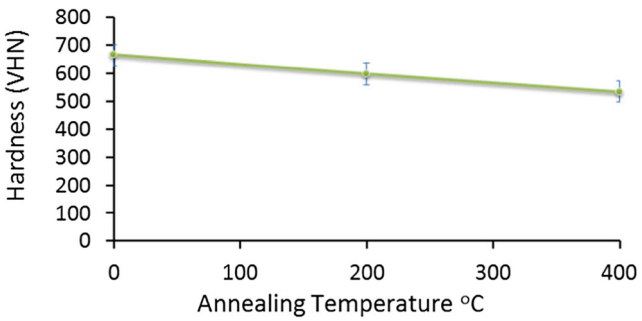


**Fig. 5** Average microhardness measurements for the $Ni/TiO_2$ coatings

decreased which is expected to reduce the wear rate. Secondly, the application of a compressive load during testing is believed to cause a work hardening effect on the coating. As the coating hardness increased, the wear resistance will also increase [32].

Figure 6a shows the wear profile for the coatings tested as a function of annealing temperature using a 10-N load. The figure shows marginal differences in the wear profile of the as-deposited coatings and the coatings annealed to 200 °C. When the coatings were annealed to 400 °C, the depth of the wear track increased significantly. Similar behaviors were observed for coatings tested at 25 N and 40 N as shown in Fig. 6b, c respectively. It is evident that the $TiO_2$ nanoparticles can effectively control the wear rate of the $Ni/TiO_2$ coating up to 200 °C. The introduction of hard $TiO_2$ nanoparticles into the Ni matrix reduces the ductility of the Ni matrix and increases the hardness without causing brittleness. This is possible because nanoparticles restrict dislocation motion in the lattice [32]

The deep wear scars observed in the coatings were attributed to the accelerated removal of particle clusters from the surface of the coating during the first stage of wear. Beyond 400 s, the samples appear to enter steady-state wear as the gradient of the curves decreases with time. Similar behavior was observed for all loading conditions tested.

A comparative view of the effect of the annealing temperature on the wear scar depth is summarized in Fig. 7a and shows that as the annealing temperature increased, the depth of the wear scar increased from 11 μm for the as-deposited coating to 82 μm for coatings annealed to 400 °C, when a load of 10 N was used. Similar behaviors were observed for coatings tested with loads of 25 N and 40 N respectively. When the effect of the load was studied, it was found that as the load increased, the depth of the wear scar also increased as shown in Fig. 7b. The reduction in the wear resistance of the coating can be credited to the modification of the coating grain sizes and nanoparticle behavior as the heat treatment temperature was increased. The increase of the grain size also causes an increase in the ductility of the material since dislocation motion becomes easier. The net effect of these changes on the

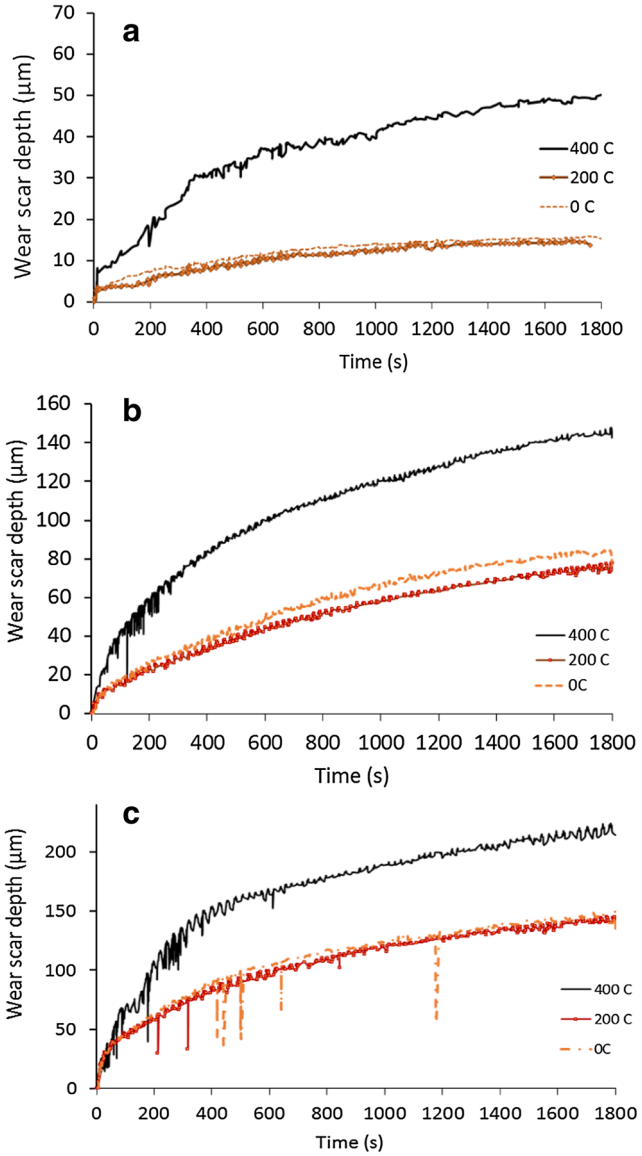


**Fig. 6** Wear profile of the Ni/$TiO_2$ coatings as a function of time and tested at **a** 10 N, **b** 25 N, and **c** 40 N respectively

mechanical performance of the coating is that the yield strength of the coating decreases which is reflected as a reduction of the hardness and wear resistance of the $NiTiO_2$ coating as was found in this study.

### 3.4.1 Effect of load on the wear rate

Analysis of the results shown in Fig. 8 indicated that the wear rates of the as-deposited coating increased from 0.009 to 0.08 μm/s when the load was increased from 10 to 40 N. When annealing temperatures of 200 °C were used, a similar behavior was observed with the wear rate increasing from 0.01 to 0.08 μm/s. For coatings heat treated to 400 °C, the wear rates increased from 0.04 to 0.12 μm/s; when the load was increased to 40 N, the wear rate increased significantly to 0.12 μm/s.

The results suggest that the mechanical performance of nanocrystalline coatings decreased significantly when the annealing temperature increased beyond 200 °C. At temperatures below 200 °C, the wear rate is less responsive to change in temperature due to the presence of the nanosized $TiO_2$ particles in the lattice. These particles exert a pinning force which is expected to retard grain growth during heat treatment [26]. Niu et al. [31] suggested that the wear rate of Ni/$TiO_2$ coating is less responsive to changes in temperature up to 200 °C, for coating containing in excess of 15 wt% $TiO_2$ nanoparticles.

### 3.4.2 Effect of heat treatment temperature on the wear rate

Figure 9 shows the effect of heat treatment temperature on the wear rate of the coatings evaluated as a function of load. When the as-deposited coating was tested, the results showed that the wear rate of the coating increased with increasing load, from 0.001 μm/s at 10 N to 0.08 μm/s at 40 N. When the coatings were heat treated to 200 °C, the wear rate of the coating similarly increased with increasing load from 0.001 μm/s at 10 N to 0.075 μm/s at 40 N. However, when wear rates of the coatings heat treated to 200 °C are compared to the wear rates of the as-deposited coatings, it was found that the heat-treated coatings recorded lower wear rates for all three loads tested. During the heat treatment, the residual micro-stress within the coatings is relieved which are expected to cause an increase of the coating's ductility. It is assumed that under the effect of the test load, the coating is work hardened, which marginally increases the wear resistance of the coating and decreases the wear rate.

Further increase of the annealing temperature to 400 °C resulted in a significant increase of the wear rate with

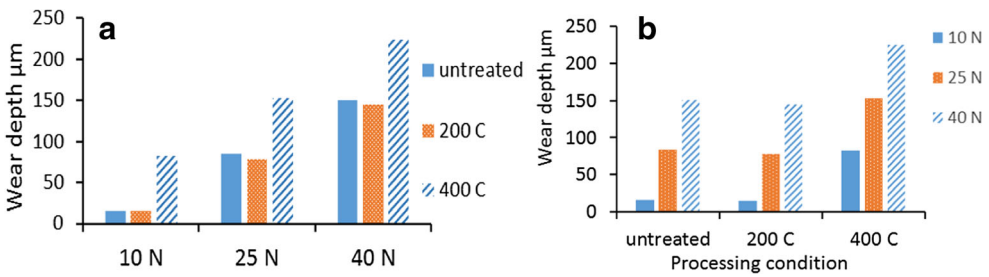


**Fig. 7** **a** Summary of the effect of heat treatment temperature on the wear scar depth. **b** Summary of the effect of load on the wear scar depth

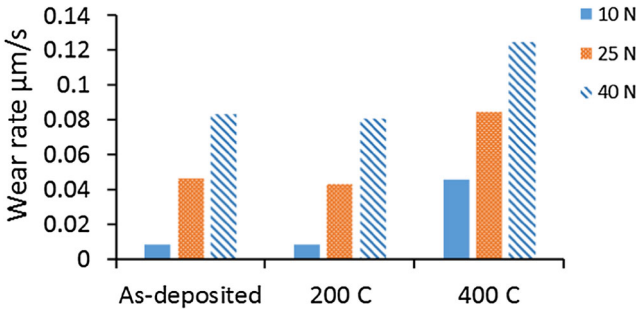


**Fig. 8** The effect of normal load on the wear rate of the Ni/$TiO_2$ coatings

increasing load from 0.04 µm/s at 10 N to 0.12 µm/s at 40 N. These changes in the wear rate were attributed to a reduction of the yield strength of the coating due to microstructural changes occurring at higher heat treatment temperature.

### 3.4.3 Analysis of wear track

Figure 10a–c presents the SEM micrograph of the wear scars for the as-deposited coatings tested at 10, 25, and 40 N respectively. Analysis of the image revealed that as the load increased, the width of the wear scar also increased with large sheet-like debris present at the edges of the wear scar for coating tested at 25 and 40 N. Additionally, the amount of wear debris on the side of the wear track appears to increase. The microcracks observed suggest that the coating is brittle in the as-deposited condition. Figure 10d–f shows that wear scars for the Ni/$TiO_2$ coatings were heat treated to 200 °C and tested as a function of load. Large sheet-like debris was observed at the edges of the wear scar and appear to increase in volume as the load was increased from 10 to 40 N. Additionally, more delaminated regions were observed in the annealed coatings, which suggest that as the heat treatment temperature increased, the ductility of the coatings also increased. The wear mechanisms appear to be a mixture of abrasive and adhesive wear.

Figure 10g–i shows the wear scars for the Ni/$TiO_2$ coatings were heat treated to 400 °C. Analysis of the images showed that the coatings appeared to have suffered severe plastic deformation due to the presence of large sheet-like debris and several delaminated regions within the wear scar for coatings

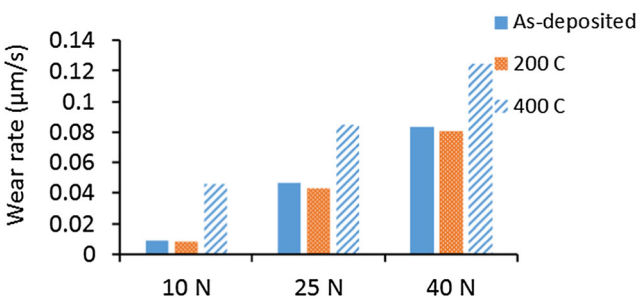


**Fig. 9** The effect of processing temperature on the wear rates of the coatings

tested at 25 and 40 N as shown in Fig. 10h. The wear mechanisms were attributed to a combination of abrasive and adhesive wear. At lower test loads, the wear mechanism appeared to be two-body abrasive wear based on the presence of parallel grooves indicative of abrasive wear

### 3.4.4 Effect of grain growth on coating performance

Grain growth is a thermally activated process; therefore as the annealing temperature increased, the expectation is that the grain size will also increase. The average grain size was determined by calculating the ASTM grain size number. The grain growth occurring in the coating can be calculated using the Grain Growth Law as shown in Eq. 2.

$$D^2 - D_o^2 = K_o t\, e^{\frac{-Q}{RT}} \tag{2}$$

where $D$ is the average grain size, $D_o$ is the size of the grain prior to heat treatment, $t$ is time, $R$ is gas constant and $T$ is the absolute temperature, $K_o$ is the rate constant, and $Q$ is the activation energy.

The addition of nanosized $TiO_2$ particle to the coating should act to restrict grain growth, as predicted by Zener pinning. Using the Zener-Smith equation, the drag effect of the particles can be determined using a force balance at the particle surface [33] to determine if the particles are capable of pinning the boundaries. The primary assumption in applying this equation is that the boundary intersects randomly with the particles. Therefore, the pinning pressure applied by the particle can be calculated using Eq. 3.

$$P_{\text{drag}} = \frac{3f\gamma}{2r} \tag{3}$$

The pressure applied to the particle due to grain growth can be estimated using Eq. 4.

$$P_{\text{grain growth}} = \frac{2\gamma}{H} \tag{4}$$

By equating the driving force of grain growth to the particle drag force, the point at which grain growth stagnates can be calculated using Eq. 5.

$$P_{\text{drag}} = P_{\text{grain growth}}$$
$$\frac{3f\gamma}{2r} = \frac{2\gamma}{H} \tag{5}$$

Equation 5 is more popularly referred to as the Zener-Smith equation in the form shown in Eq. 6.

$$H_{\max} = \frac{4r}{3f} \tag{6}$$

where $H$ is the maximum diameter of the grain size that can be stopped by a particle of radius $r$, $f$ is the particle volume

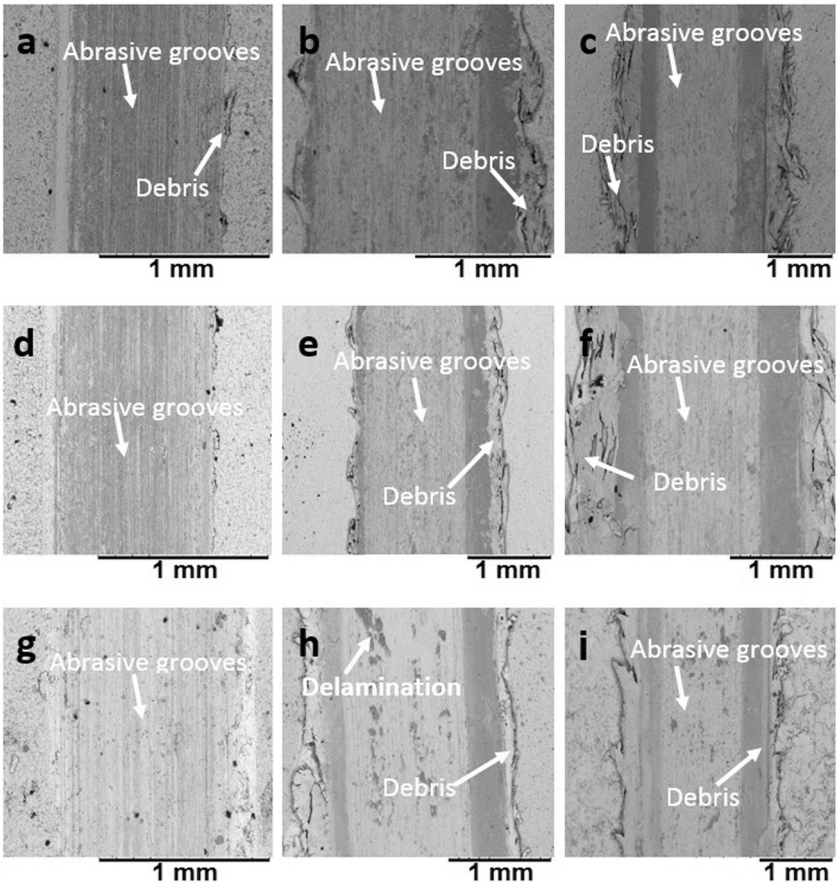


**Fig. 10** SEM micrograph of the wear tracks for the nanocrystalline Ni/$TiO_2$ coatings. As-deposited tested: **a** 10 N, **b** 25 N, and **c** 40 N. Annealed to 200 °C: **d** 10 N, **e** 25 N, and **f** 40 N. Annealed to 400 °C: **g** 10 N, **h** 25 N, and **i** 40 N

fraction in the material, and $\gamma$ is the grain boundary energy. From the data collected in the study, the diameter of the particle used in the study was 40 nm and the measured volume fraction of particles deposited in the coating was 0.164. Using this information, the maximum grain size at the stagnation point was calculated to be 162.6 nm.

When the calculated grain size was compared to the measured grain size, it was found that for coatings annealed to 200 °C, the grain size in the coating was measured to be approximately 435.5 μm while for coatings annealed to 400 °C, it recorded a grain size of approximately 873.8 μm. The results calculated using the Zener-Smith equation confirm that grain growth is responsible for the reduction of the coating hardness and subsequent increase of the wear rate as the annealing temperature was increased. Grain growth leads to the nanoparticles segregating to the grain boundary regions of the coating, which reduces the ability of the particles to impede dislocation motion.

## 4 Conclusions

This study evaluated the effects of heat treatment on the tribological behavior and thermal of Ni/$TiO_2$ nanocrystalline coatings produced by electrophoretic deposition and permits a clear understanding of the impact of heat treatment temperature on the strengthening behavior of nanosized reinforcements on coating properties.

XRD analysis indicated that the inclusion of nanosized $TiO_2$ particles into the Ni matrix had a significant effect on the microstructure and mechanical performance of the coating. When the heat treatment temperature increased, the sharpness of the XRD peaks also increased, which suggests the removal of residual stresses from the coating and an increase of grain size. The microstructural changes were subsequently confirmed by microhardness measurements which showed that coating hardness decreased with increasing annealing temperature. Further analysis of the mechanical performance of the coatings using pin-on-plate wear testing shows that the wear rate of the coating increased with both load and heat treatment temperature.

Numerical analysis of the grain growth and grain boundary pinning using the Zener-Smith equation showed that the changes observed in the mechanical behavior of the coatings can be attributed to thermally activated grain growth which caused segregation of the $TiO_2$ nanoparticles to the grain boundary regions. The clustering of the $TiO_2$ nanoparticles into the grain boundaries reduced the effectiveness of the particles to impede dislocation motion, which caused a reduction of both the hardness and the wear resistance of the coating.

## Compliance with ethical standards

**Conflict of interest** The authors declare that they have no conflict of interest.



## References

1. A. Jung, H. Natter, R. Hempelmann, E. Lach, Nanocrystalline alumina dispersed in nanocrystalline nickel: enhanced mechanical properties. J. Mater. Sci. **44**, 2725–2735 (2009)
2. L. Chen, L. Wang, Z. Zeng, J. Zhang, Effect of surfactant on the electrodeposition and wear resistance of Ni–Al2O3 composite coatings. Mater. Sci. Eng. A. **434**, 319–325 (2006)
3. K. Sheng-Lung, J. Chin. Inst. Eng. **28**(1), 1–8 (2005)
4. G. Parida, D. Chaira, M. Chopkar, A. Basu, Synthesis and characterization of Ni-TiO2 composite coatings by electro-co-deposition. Surf. Coat. Technol. **205**(21–22, 25), 4871–4879 (2011)
5. G. Wu, N. Li, D.R. Zhou, K. Mitsuo, Electrodeposited Co–Ni–Al2O3 composite coatings. Surf. Coat. Technol. **176**, 157–164 (2004)
6. C. Guozhong, (Imperial College Press, London, 2004)
7. C.T.J. Low, F.C. Walsh, Self-lubricating metal composite coatings by electrodeposition or electroless deposition. Encyclopedia of Tribology, 3025–3031 (2013)
8. T. Moritz, W. Eiselt, K. Moritz, Electrophoretic deposition applied to ceramic dental crowns and bridges. J. Mater. Sci. **41**, 8123–8129 (2006)
9. K.H. Hou, M.D. Ger, L.M. Wang, S.T. Ke, The wear behaviour of electro-codeposited Ni–SiC composites. Wear **253**, 994–1003 (2002)
10. I. Garcia, J. Fransaer, J.-P. Celis. Surf. Coat. Technol. **148** 171–178 (2001)
11. L. Peraldo, B. Benedetto, B.C. Mele, L. D'Urzo, Int. J. Electrochem. Sci. **3**, 356–408 (2008)
12. D.E. Rusu, P. Cojocaru, L. Magagnin, C. Gheorghies, G. Carac, J. Optoelectron. Adv. Mater. **12**(12), 2419–2422 (2010)
13. L. Besra, M. Liu, A review on fundamentals and applications of electrophoretic deposition (EPD). Prog. Mater. Sci. **52**, 1–61 (2007)
14. K.O. Cooke, in *Electrodeposition of composite materials*, ed. by A. M. A. Mohamed. Parametric analysis of electrodeposited nanocomposite coatings for abrasive wear resistance (Intech, 2016). https://doi.org/10.5772/62153
15. S.A. Abdel Gawad, A.M. Baraka, M.S. Morsi, M.S. Ali Eltoum, Int. J. Electrochem. Sci., 1722–1734 (2013)
16. A. Akarapu, Thesis, (National Institute of Technology, Department of Metallurgical & Materials Engineering, Rourkela, 2011)
17. S.T. Aruna, V.E. Selvi, W.V. Grips, K.S. Rajam, J. Appl. Electrochem. (41), 461–468 (2011)
18. W. Sun, M. Tian, P. Zhang, H. Wei, G. Hou, Y. Wang, **69**(8), 1501–1511 (2016)
19. C.R. Raghavendra, S. Basavarajappa, I. Sogalad, J. Mater. Sci. Eng. **149**, 012110 (2016). https://doi.org/10.1088/1757-899X/149/1/012110
20. P. Gadhari, P. Sahoo, Procedia Mater. Sci. **6**, 623–632 (2014)
21. E. Saraloğlu Güler, in *Electrodeposition of composite materials*, ed. by A. M. A. Mohamed. Effects of electroplating characteristics on the coating properties (InTech, 2016). https://doi.org/10.5772/61745
22. L.N. Bengoa, P. Pary, W.A. Egli, Codeposition of particles: role of adsorption of the electroactive species. J. Electrochem. Soc. **163**(14), 780–786 (2016)
23. M. Stroumbouli, P. Gyftou, E.A. Pavlatou, N. Spyrellis, Surf. Coat. Technol. **195**(2–3, 31), 325–332 (2005)
24. M.A. Farrokhzad, T.I. Khan, Surf. Coat. Technol. **304**(25), 401–412 (2016)
25. B.E. Conway, C.G. Vayenas, R.E. White, M.E. Gamba Adelco, *Modern aspects of electrochemistry*, vol 38 (Kluwer Academic/Plenum Publishers, New York, 2005)
26. S.C. Wang, W.C.J. Wei, Characterization of electroplated Ni/SiC and Ni/Al2O3 composite coatings bearing nanoparticles. J. Mater. Res. **18**(7), 1566–1574 (2003)
27. A.I. Pavlov, L. Benea, J.-P. Celis, L. Vazquez, Dig. J. Nanomater. Biostruct.**8**(3), 1043–1050 (2013)
28. K.O. Cooke, Metall. Mater. Trans. B, 627–634 (2012)
29. R. Chaim, Grain coalescence by grain rotation in nano-ceramics. Scr. Mater. **66**(5), 269–271 (2012)
30. H. Sarma, K.C. Sarma, International Journal of Scientific and Research Publications **4**(3, ISSN 2250–3153) (2014)
31. T. Niu, W. Chen, H. Cheng, L. Wang, Trans. Nonferrous Metals Soc. China, 272300–272309 (2017)
32. K. Kato, Wear in relation to friction — a review. Wear **241**, 151–157 (2000)
33. P.A. Manohar, M. Ferry, T. Chandr, Five decades of the Zener equation. ISIJ Int. **38**(9), 913–924 (1998)